ANL-6915

ANL-6915

Argonne National Laboratory

FLUX TRAP EXPERIMENTS IN D_2O-MODERATED THORIA-URANIA CORES

by

K. E. Plumlee

Printed in USA. Price $2.00. Available from the Clearinghouse for Federal Scientific and Technical Information, National Bureau of Standards, U. S. Department of Commerce, Springfield, Virginia

ANL-6915
Reactor Technology
(TID-4500, 37th Ed.)
AEC Research and
Development Report

ARGONNE NATIONAL LABORATORY
9700 South Cass Avenue
Argonne, Illinois 60440

FLUX TRAP EXPERIMENTS IN D_2O-MODERATED THORIA-URANIA CORES

by

K. E. Plumlee

Reactor Physics Division

October 1964

Operated by The University of Chicago
under
Contract W-31-109-eng-38
with the
U. S. Atomic Energy Commission

TABLE OF CONTENTS

TABLE OF CONTENTS

LIST OF FIGURES

LIST OF TABLES

FLUX TRAP EXPERIMENTS IN D_2O-MODERATED THORIA-URANIA CORES

by

K. E. Plumlee

ABSTRACT

Experiments are reported involving 25 D_2O and three small H_2O internal thermal columns (ITC), or flux traps, inside annular thoria-urania cores. The moderator and the radial reflector were D_2O. Several different fuel densities were used. ITC's were as large as 104 x 104 cm. Radial activation plots indicated central peaks up to ten times the fuel zone average at the midplane, and five times the fuel zone maximum. Available fuel and facilities were used to obtain data for evaluation of computational methods, which were reported separately. The limited selection of fuel prevented optimization of experimental cores.

I. INTRODUCTION

Several D_2O and H_2O-D_2O thermal flux trap cores were assembled in the ZPR-VII Critical Facility during 1959. Portions of the data obtained in these cores have been presented in preliminary reports.[1,2] This report provides a comprehensive account of the experimental measurements made with flux trap configurations during the Thoria-Urania-Deuterium (THUD) Critical Experiment.[3]

A subsequent experiment, which has already been reported,[4-6] utilized an H_2O flux trap, an H_2O moderator, highly enriched uranium fuel, and a peripheral beryllium reflector. Currently there are plans to perform a critical experiment with a more heavily loaded core of improved design[7] producing a nearly epithermal spectrum in the fuel zone.

The assemblies of this report included a wide range of fuel loading densities and configurations. The existing fuel and grids of the THUD experiment were used although a few fixtures were specially fabricated for flux trap work. These included aluminum thimbles to contain internal (axial) H_2O thermal columns, foil holders, and similar items. Further work with fuel and geometry designed for the experiment might add significantly to the available information.

Calculations made after the experiment were reported in Reference 1. That report verified the experimental evidence that critical assemblies could be made using a single, densely loaded, annular, fuel zone with relatively low resonance escape probability (P), having $K_\infty < 1$, if properly reflected by internal and external D_2O regions. (Fuel worth was negative for all fuel zone thicknesses exceeding ~4 cm.) Material constants, calculated critical dimensions, and calculated fluxes were given in that report. A typical core is shown in Fig. 1.

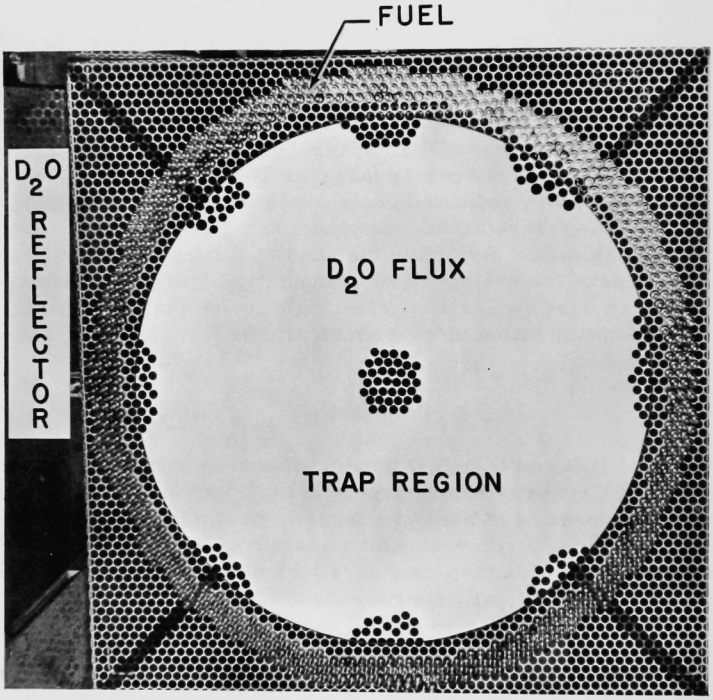

112-4432

Fig. 1. Photograph of ~3-cm-thick, Annular Fuel Zone Enclosing a Flux Trap

Experimental measurements in clustered and in uniform lattice cores using the same fuel, moderator, and facilities were reported in Reference 3. General information given in the reference has not been duplicated in this report unless directly involved in calculations or adjustments.

For readers not familiar with thermal flux trap reactors, the following general description is given of a flux trap design, its advantages, and some suggested uses thereof. This may clarify the purpose of some of the experimental work. A quite large thermal flux peak can be obtained by building an annular fuel zone enclosing a central moderator region (sometimes called a water gap, an internal thermal column, a flux trap, or an internal reflector). In comparison to external reflector flux peaks, the internal peak or flux trap may receive leakage neutrons from two or more directions instead of one; consequently, the flux peak may be considerably more abrupt in the flux trap design. In addition to annular core designs, there have been suggestions to sever the annulus at the midplane, or to use spherical, hemispherical, or segmented fuel region shells.

Prospective advantages of flux traps are as follows: (a) If a central flux trap appears sufficiently large and accessible for the highest-level irradiations envisaged, the power and fuel requirements of a research reactor or irradiation reactor may be minimized by using a flux trap. An external reflector may still provide a large region of less intense flux for other irradiations. (b) It may be possible to increase the maximum flux available for beams and irradiations by installing a flux trap in a core that is limited to a given maximum in the fuel zone by reactivity, coolant temperature, or heat transfer problems. (c) The magnitude of the thermal flux may be increased greatly, relative to that of the epithermal flux, by using a flux trap of appropriate design.

Potential uses for flux traps include the following: Extremely high thermal fluxes are needed to provide beams of high intensity, to produce short-lived isotopes, and to irradiate samples which are in very limited supply or have short half-lives. Some experiments require a maximum of thermal flux but a minimum of epithermal flux to avoid contaminants produced by reactions attributed to the fast and epithermal flux components normally associated with nuclear reactors. Flux traps may be designed to meet such requirements.

II. SUMMARY

Measurements were made with a wide range of flux trap dimensions inside thoria-urania-fueled cores, which were moderated and reflected by D_2O. Roughly 25 D_2O-filled, and three small H_2O-filled, axial flux traps were constructed. The flux trap dimensions ranged up to 104 x 104 cm. Fuel zones ranged from very dense to very dilute loadings, and from very thin (2.8-cm-thick annular fuel region) to broad (95-cm radius) regions. Resonance absorption was strong because of the limited selections of fuel.

Activation peaks in radial traverses at the midplane were as high as ten times the two-dimensional average through the fuel zone, five times the maximum in the fuel zone, and three times the external reflector peak.

The greatest peaks were with relatively thin, but densely loaded, fuel annuli. The cadmium ratios of foil materials increased significantly as the size of the flux traps increased. Consequently, part of the activation peak may be attributable to a shift in the neutron energy spectrum.

An increase in reactivity accompanied fuel removal from the axis of cylindrical cores, because of the effect of resonance absorption. This gain in reactivity was so pronounced in a tight lattice that criticality was obtained with very densely loaded fuel zones having K_∞ less than unity. Removal of the centermost 767 fuel elements from a subcritical cylindrical core containing 1482 fuel elements was sufficient to obtain criticality. Reactivity was correlated with both the thickness of the annular fuel zone (with an optimum between 3.5 and 4.0 cm for the case cited) and the radius of the flux trap. In all cores, reactivity increased as the radii of D_2O flux traps were increased, up to 6 cm or larger.

Experimentation with H_2O axial flux traps inserted into (or replacing) D_2O traps was limited to 5.1-cm radius and less. Flux peaking was greater in H_2O traps than in D_2O traps in the same cores. However, no H_2O trap was installed in the most densely loaded lattice, which produced the greatest peaks measured in D_2O traps. A considerable loss of reactivity was associated with installation of the larger, H_2O-filled thimbles. Consequently, work with H_2O traps was quite limited because of difficulty in loading to criticality, and because safety aspects were more severe.

Reactivity worth of incremental increases in D_2O height ($d\rho/dH$) was not greatly affected by installation of flux traps in several of the cylindrical cores. The largest change noted was an increase of ~10% in the $d\rho/dH$ of a core with 30.5-cm radius flux trap, as compared with cylindrical cores having the same fuel spacing. Since $d\rho/dH$ measurements may be used to indicate migration areas, it was not clear why the D_2O flux traps did not greatly affect this characteristic since they occupied a region of high importance.

The available fuel consisted of 152-cm column lengths of ceramic thoria-urania pellets in aluminum tubing. The two varieties had 15/1 and 25/1 atomic ratios (Th/U^{235}). Pellet radii were 0.33 and 0.30 cm. The tubing had inner and outer radii of 0.36-0.40, and 0.31-0.39 cm, respectively. Fuel elements were positioned by insertion through grid plates having openings 0.95 cm center-to-center in a triangular pattern. Fuel elements were spaced in multiples of 0.95 cm (or A_0) from 0.95 through 5.71 cm ($6A_0$), and the measurements involved 0.95, 1.90, 2.85, and 5.71-cm triangular-spaced lattices. D_2O purity ranged downward from an initial value of 97.8% to a final value of 97.2% because of exchange with atmospheric moisture.

Fuel containing a large amount of parasitic absorber (ThO_2) was used because of its ready availability, and the need of data for evaluation of computational methods.

Although the fuel zones conserve fissionable material, because of their conversion ratios (~0.3 to ~0.6), the power levels extrapolate (for the better cores) to 360-450 MW for 10^{16} thermal neutron flux intensity in the flux trap. The large size feasible with D_2O flux traps may prove sufficiently attractive to offset the relatively high power levels involved. Improved outlook may result from better fuel and geometry. These assemblies have peculiarities that may prove to be useful. Void worth was negative in all cases measured, whereas light-water systems may have regions of both positive and negative void worth. Samples inserted on the axis of large flux traps had no measurable effect on reactivity. Rather large traps could be constructed with little loss of reactivity.

III. FOIL ACTIVATION TRAVERSES

A. Radial Peak-to-average Ratios

Activation peaks as large as ten times the average in the fuel zone were obtained in radial activation plots (Figs. 2 to 5). Table I lists the radial peak-to-average activations, fuel zone dimensions, run numbers,

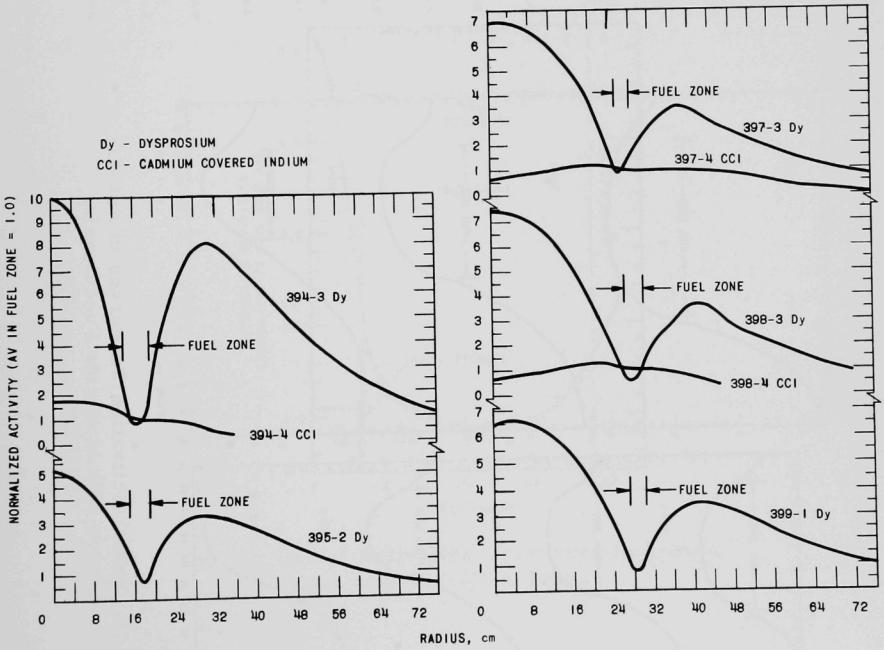

Fig. 2. Radial Activation Traverses in Annular Cores with High Fuel Density

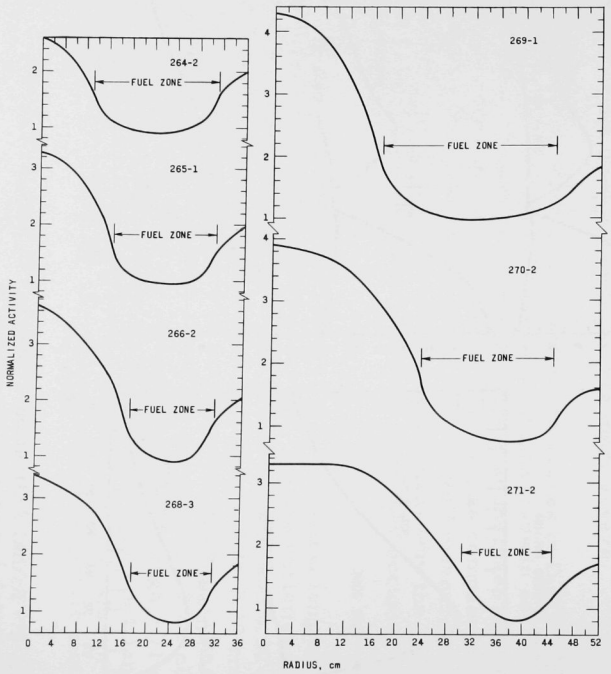

Fig. 3. Radial Activation Traverses in Annular Cores with Moderate Fuel Density

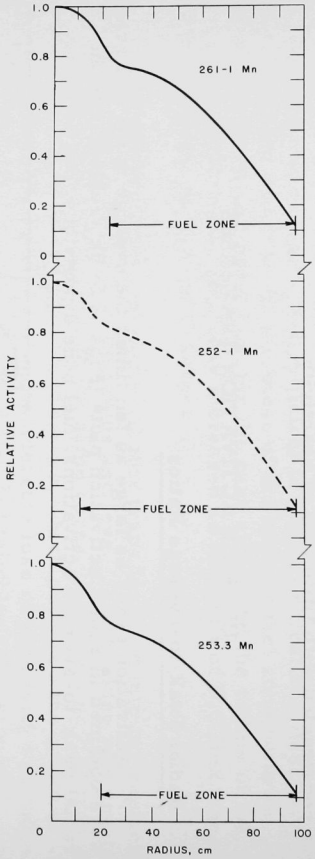

Fig. 4

Radial Activation Traverses in Annular Cores with Low Fuel Density

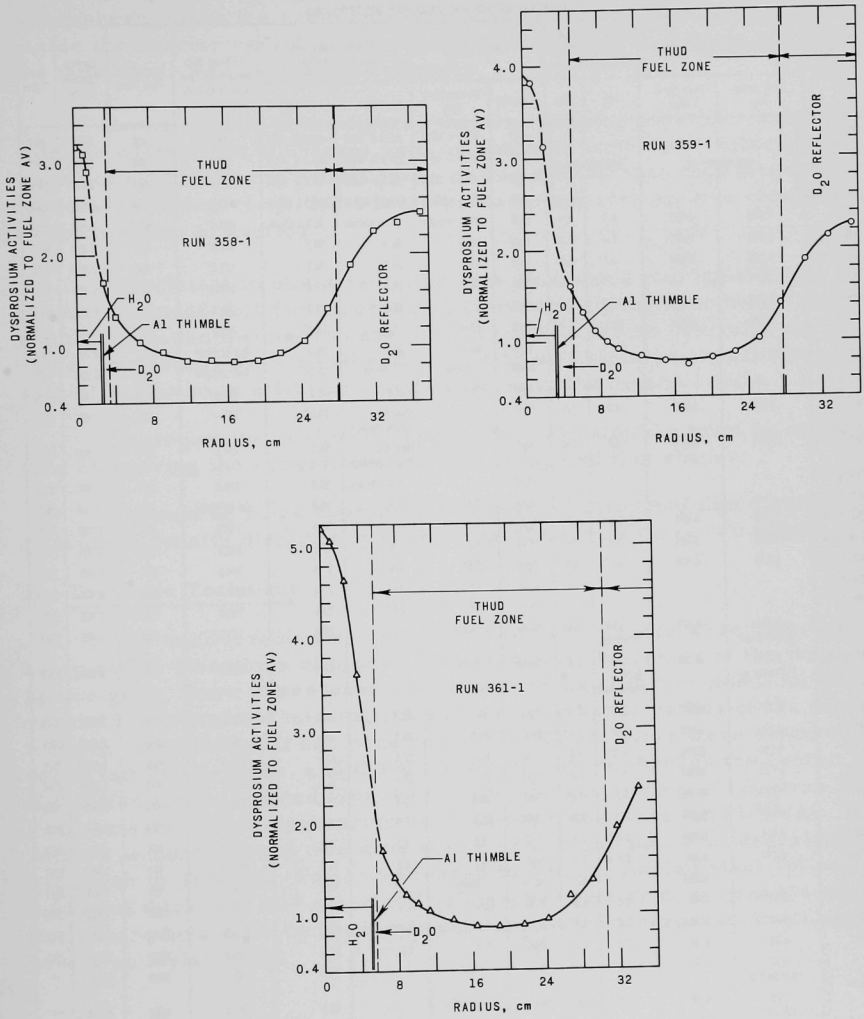

Fig. 5. Radial Activation Traverses in Annular Cores with H_2O Flux Traps

Table I

ACTIVATION RATIOS AND ASSEMBLY DESCRIPTIONS

Loading & Run No.	Approx ϕ Peak / Specific Power*		Ratios of Peak Activity to Mid-plane Fuel Zone		Flux Trap		Approx Fuel Zone Dimensions (cm)		Critical D_2O Height in Fuel and Trap (cm)	Number of Fuel Pins	Lattice Spacing (cm)	Fuel Type
	Fuel Zone Avg	Fuel Zone Max	Avg	Max	Material	Dimensions (cm)	Inner	Outer				
449-1, -4	Not measured		Not measured		D_2O	67.9 x 67.9	67.9 x 67.9	83.8 x 83.8	148.8+	488	1.905	15/1
448-1					D_2O	64.6 x 64.6	64.6 x 64.6	83.8 x 83.8	116.1	588	1.905	15/1
447-1, -2					D_2O	63.5 x 63.5	63.5 x 63.5	83.8 x 83.8	107.7-	624	1.905	15/1
446-1, -2					D_2O	104.0 x 104.0	104.0 x 104.0	124.5 x 124.5	142.3	936	1.905	15/1
399-1	0.033	0.023	6.9	4.9	D_2O	27.7- radius	27.7- radius	30.5 radius	115.9-	670	0.953	15/1
398-1, -3	0.035	0.025	7.4	5.3+	D_2O	26.9	26.9	30.5	108.6-	840	0.953	15/1
397-1, -4	0.032	0.026	6.7-	5.4	D_2O	25.4	25.4	28.1	118.5-	568	0.953	15/1
396-1	-	-	-	-	D_2O	16.4	16.4	19.3-	141.2	403	0.953	15/1
395-1, -2	0.025	0.015	5.2	3.2	D_2O	15.3	15.3	19.3-	135.9	550	0.953	15/1
394-1, -4	0.048	0.019	10.0	4.0	D_2O	13.8	13.8	19.3-	145.2	715	0.953	15/1
393-1	-	-	-	-	D_2O	10.6	10.6	19.3-	Not critical	1032	0.953	15/1
391-1	-	-	-	-	None	None	None	19.3-	Not critical	1482	0.953	15/1
374-1, -2	-	-	-	-	D_2O	~28.0	~28.0	~41.0	147.8-	739	1.905	25/1
367-1, -2	0.154	0.052	4.4	1.5	H_2O	5.1	Hex. 5.6- equiv. radius	29.0+	161.9	812	1.905	25/1
365-1	0.164	0.070	4.7	2.0	H_2O	5.1	Hex. 5.2 equiv. radius	30.5	139.1	893	1.905	25/1
364-1, -6	-	-	-	-	H_2O	5.1	5.6- radius	30.5	138.2	899	1.905	25/1
363-1	-	-	-	-	H_2O	7.6	~7.9	30.8	Not critical	925	1.905	25/1
361-1, -4	0.182	0.091	5.2	2.6	H_2O	5.1	5.6-	30.5	137.0	899	1.905	25/1
359-1, -2	0.136	0.084	3.9-	2.4+	H_2O	3.2	4.4	27.6	140.9	743	1.905	25/1
358-1, -3	0.112	0.066	3.2-	1.9-	H_2O	2.5+	2.6+	27.6	132.6	755	1.905	25/1
357-2	-	-	-	-	Void	2.5+	2.6+	27.6	137.4	755	1.905	25/1
357-1	-	-	-	-	D_2O	2.6+	2.6+	27.6	131.7	755	1.905	25/1
356-1, -2	0.031 (central ϕ)	0.021	0.88 (central)	0.61	None	None	-	27.6	133.2+	762	1.905	25/1
	0.070 (reflector ϕ)	0.049	2.0 (radial reflector)	1.4	None	None	-	27.6	133.2+	762	1.905	25/1
271-2	0.115	0.080	3.3+	2.3-	D_2O	30.5	30.5	44.5	123.2	970	1.905	25/1
270-2	0.136	0.080	3.9-	2.3-	D_2O	23.7	23.7	44.5	91.0-	1268	1.905	25/1
269-1	0.150	0.098	4.3+	2.8	D_2O	17.1	17.1	44.5	76.8-	1526	1.905	25/1
268-3	0.112	0.084	3.2-	2.4	D_2O	17.1	17.1	31.1	137.2-	651	1.905	25/1
266-2	0.129	0.076	3.7	2.2+	D_2O	16.2	16.2	31.1	118.6	743	1.905	25/1
265-1	1.115	0.070	3.3	2.0	D_2O	12.9	12.9	31.1	108.0-	829	1.905	25/1
264-2	0.091	0.066	2.6+	1.9	D_2O	9.3	9.3	31.1	103.1	901	1.905	25/1
263-2	0.070	0.049	2.0	1.4	D_2O	4.3	4.3	31.1	103.3-	953	1.905	25/1
262-2	-	0.059	-	1.7	None	None	-	31.1	104.5	977	1.905	25/1
261-1	0.78**	0.42	2.4	1.3-	D_2O	11.1	11.1	99.0	122.7	1047	5.715	25/1
253-3	0.78**	0.36	2.4	1.1+	D_2O	8.2+	8.2+	99.0	113.5	1064	5.715	25/1
252-1	0.78	0.36	2.4-	1.1-	D_2O	5.4	5.4	99.0	108.2	1076	5.715	25/1
251-3	0.32 (central ϕ)	0.32	1.0	1.0+	None	None	-	99.0	105.3	1082	5.715	**
	0.72 (reflector ϕ)	0.32	2.2	1.0+	None	None	-	99.0	105.3	1082	5.715	**

*Ratio of estimated thermal flux in flux trap peak to fissions per liter-second in the fuel region, at the midplane.
**Calibrated measurements of thermal flux intensity and fission rate. See Section IV of this report.

and criticality measurements. The fuel types, lattice spacing, and trap compositions are also given. All cores were assembled in a 103-cm, inside-radius vessel which was filled with D_2O to the indicated heights during critical dimension measurements. Moderator purity was estimated

to be between 97.8% D_2O initially (lower run numbers in Table I) and 97.2% finally. The change was attributed to moisture exchange with the atmosphere, since the room was ventilated by intake from outdoors. Air inside the reactor vessel and the dump tank diffused with room air while the tank cover was off for core changes.

It was notable in the figures that flux peaking generally increased with the width of the D_2O traps until an optimum occurred. Although plots were not made with the widest traps, it was evident that such large central moderator regions provided a large subcadmium activation in comparison to epicadmium activation.

An attempt to plot a radial neutron flux shape was considered, but it was concluded that the uncorrected activation distribution would be more useful. Because the neutron energy distribution varied radically along radial traverses, the activation distribution was affected significantly by spatial variation in effective cross sections of the detector foils.

Consequently, it should be noted that adjustments must be made before comparing the activation plots with computed flux shapes.

It would be more appropriate to convert computed flux distributions to neutron density distributions for comparison with these two plots.

B. Traverse Technique

For each irradiation, two or more foil traverses were inserted along radial directions of approach (six) toward the center of the triangular lattice grid. Some cores were loaded with an axial lattice position, which resulted in traverses missing the exact center by the radius of the central fuel pin (even though it had been removed). Other cores were centered between lattice positions, and these traverses passed through the center. The H_2O-filled traps included fixtures for precise positioning of traverse foils. Foil materials were dysprosium-aluminum, manganese, and U^{235}-Al. A limited amount of work was done with gold and indium. Foil descriptions are given in Table II. Foils were taped to long, enameled steel splines 0.015 cm thick and 1.27 cm wide (Lufkin steel rule replacement blade). Foils were held down by Mystic-brand tape which incorporated silicone adhesive on Mylar strip.

Table II

FOIL DESCRIPTIONS

Material	Composition	Size (cm)	Thickness (cm)	Weight (g)
Au	Pure	1 x 1 & 0.584 d	0.0025	0.049 & 0.0145
Dy-Al	3.7% Dy	0.584	0.0023	0.017 ± 0.001
Cu	Pure	1 x 1 & 0.584 d	0.0025 & 0.005	0.021 & 0.0055
In	Pure	0.584 d	0.0127	0.029 ± 0.003
Mn-Cu	90% Mn	0.584 d	0.0086	0.015^{+}
Enriched U	93.2% U^{235}	0.584 d	0.0025 & 0.0127	0.012 & 0.057

C. Foil Data Handling

Foil activations were counted and recorded by automatic equipment.[8] The recorded data were corrected for counter dead time, background, and decay (standard decay constants were applied, where available) by the IBM-704 computer using the ANL-807/RE-202 (FORTRAN) code, which produced both tabulated and plotted data. U^{235} fission product activities were decay-corrected by use of concurrently counted normalizing foils, utilizing approximately 1 MeV discrimination and integral count with 5-cm-dia x 5-cm-thick NaI(Tl) (Harshaw brand) scintillators. The majority of the β-emitting foils were β-counted using Pilot-B brand, thin (0.08-cm), plastic scintillators covered by 0.01-cm-thick aluminum foil.

The traverse plots were superimposed and averaged (visually) to aid in eliminating discrepancies arising from counting errors, fuel boundary irregularities, and flux tilt. Because of the steep radial gradients, scattering was noticeable. The main interest was in determining the flux trap peaks and the average activation levels of the foils in the fuel zone, which did not depend heavily on the gradients.

Traverse data were not corrected for flux depression caused by the foils or the splines to which they were attached. Since traverses passed between fuel pins, the foil activations always were in the moderator.

The flux trap region produced large cadmium ratios (i.e., indicating a soft thermal spectrum), while the fuel zones produced low cadmium ratios (hardened spectrum). The epicadmium flux component decreased as a function of distance from the fuel zone. Consequently the change in neutron cross section was significant within the length of a traverse, even for foils of identical weight and size.

D. Effect of Flux Trap Radius on Radial Activation Distributions

1. Least Densely Loaded Fuel Zone ($6A_0$ lattice spacing)

Data taken with $6A_0$ lattice spacing in the fuel zone are plotted in Fig. 6. The fuel annulus was quite thick because of reactivity requirements, and only a thin, peripheral, D_2O reflector remained between the fuel and the reactor vessel.

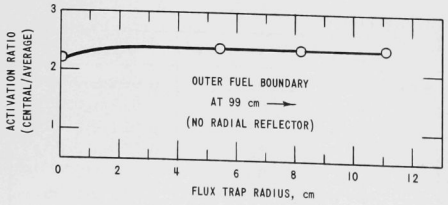

Fig. 6

Effect of Flux Trap Radius on Activation Distribution of Cores with Low Fuel Density

The enlarged, D_2O, flux trap radius resulted in increased flux peaking, throughout the range of the experiment. However, the major improvement was obtained in the first few centimeters radius. Further enlargement produced little improvement.

2. Intermediate Loading Density in Fuel Zone ($2A_0$ lattice spacing)

Data taken with $2A_0$ lattice spacing in the fuel zone are plotted in Fig. 7. The flux trap peak was affected by the radius of the trap and by the thickness of the annular fuel region.

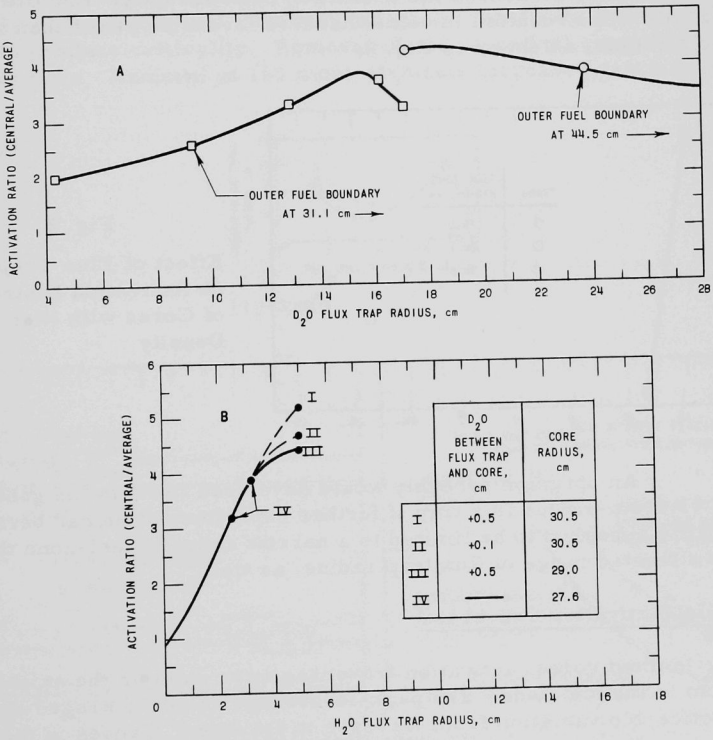

Fig. 7. Effect of Flux Trap Radius on Activation Distribution of Cores with Moderate Fuel Density

With D_2O flux traps, the activation peak increased as the radius of the trap increased, up to 17 cm. An abrupt decrease occurred at smaller radii because of unduly thin fuel zones, which were predominating effects. Loading thicker fuel zones increased the flux peak obtained with the same flux trap radius.

With H_2O flux traps, a more abrupt increase in the central peak was found with increased radius than in the D_2O traps. The effect of loading a thicker fuel zone was noticeable with an H_2O flux trap radius of 5.1 cm and fuel zone thicknesses of 24-25 cm.

3. Most Densely Loaded Fuel Zone (A_0 lattice spacing with 15/1 fuel)

The smallest flux trap radius for which criticality was obtained was 13.8 cm. The activation peak was ten times the average activation of the traverse through the fuel zone. Increasing the flux trap radius thinned the fuel zone and decreased the activation peak abruptly. Enclosure of larger flux traps resulted in somewhat less favorable peaks than with 13.8-cm radius, as shown in Fig. 8.

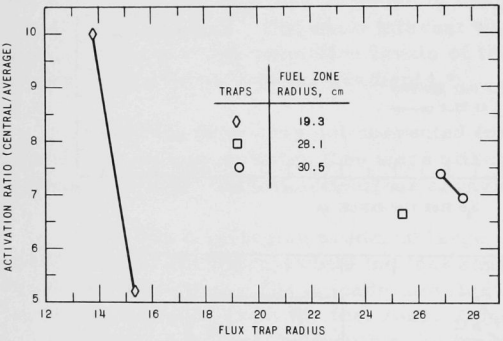

Fig. 8

Effect of Flux Trap Radius on Activation Distribution of Cores with High Fuel Density

An optimum probably would have been found in the general range of the 13.8-cm-radius flux trap if further experimentation had been done. Criticality appeared to be limited to a narrow range of fuel-zone thickness and to a limited range of flux trap radius, as well.

E. Axial Activation Traverses

In most cores, activation traverses were made in the axial position and also in the fuel zone. The peak-to-average values averaged about 0.72, with noticeable variation from traverse to traverse. Causes of this variability were thought to be the bottom reflector and the change in moderator depth from core to core. Difficulty in experimentation was encountered because of steep gradients in the vicinity of the traverses.

IV. RELATION OF FLUX TRAP RADIUS AND REACTIVITY

Reactivity was increased by removal of fuel near the axis of cylindrical cores, up to a flux trap radius of 6 cm or greater. This effect was more noticeable with the more reactive fuel and with the more densely loaded fuel zones (see Figs. 9 to 12). The optimum flux trap size, reactivity-wise, was generally smaller with the thinner fuel zones; however, the most densely loaded core was exceptional.

In the most densely loaded cores ($1A_0$ lattice cores fueled by 15/1 fuel), experimentation included loading 1482 identical fuel elements into a 19.3-cm-radius cylinder, which proved to be subcritical. Removal of the 450 center-most fuel elements increased reactivity, but not sufficiently to produce criticality. Removal of 317 more fuel elements produced a critical core. Removal of 165 more elements increased reactivity still further.

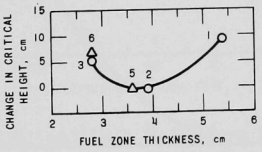

112-4429

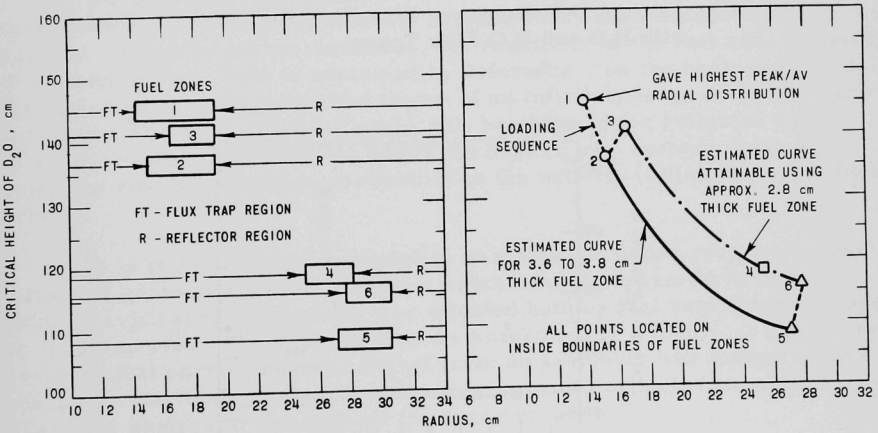

112-4431

Fig. 9. Critical D_2O Height vs Flux Trap Radius (15/1 Fuel $1A_0$)

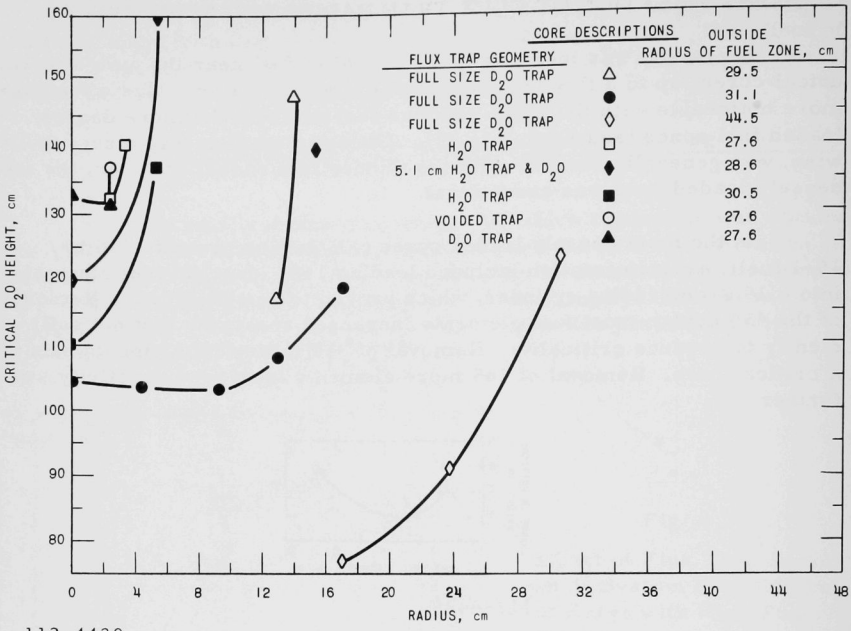

112-4430

Fig. 10. Critical D_2O Height vs Flux Trap Radius (25/1 Fuel $2A_0$, with H_2O and D_2O Flux Traps)

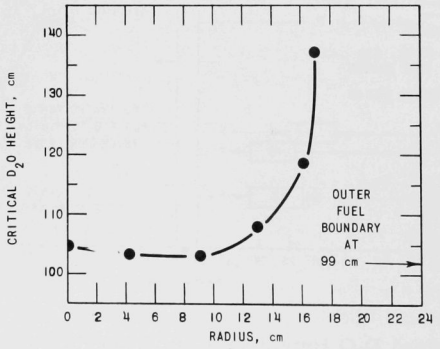

Fig. 11. Critical D_2O Height vs Flux Trap Radius (25/1 Fuel $6A_0$)

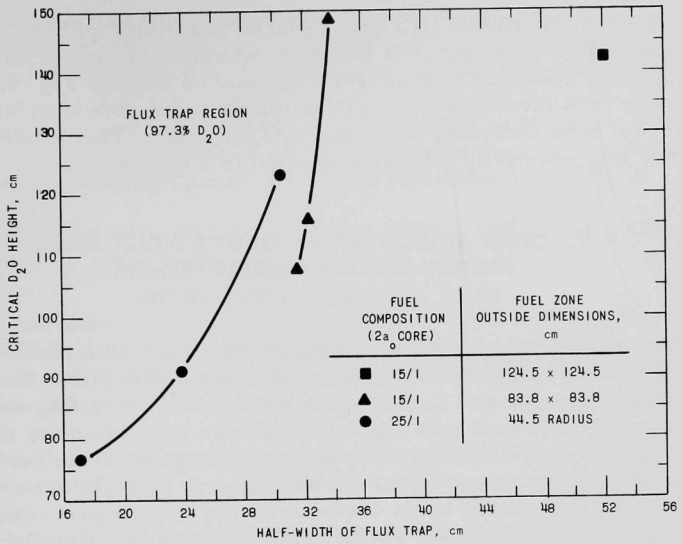

Fig. 12. Critical D_2O Height vs Half-width of Flux Trap (Wide Traps)

Further experimentation with the densely loaded fuel zone indicated that there was a strong relationship between fuel zone thickness and reactivity. At 3.5 to 4.0 cm thickness, the reactivity of the fuel zone appeared to be maximized. This is explained in Reference 1 on the basis that k_∞ for the fuel zone, the multiplication factor of an infinitely large core, was less than unity, but that criticality could still be obtained for reflected cores, in a limited range of geometry where the ratio k_∞/p_∞ exceeds unity, p_∞ being the resonance escape probability in the uniform (infinitely large) fuel zone.

It is to be noted that criticality was obtained under restricted conditions of geometry, with a fuel zone which initially appeared to be incapable of criticality. Reactivity was affected both by fuel zone thickness and by flux trap size. Whenever resonance absorption is a factor, it can not be assumed that partial removal of fuel from an assembly will always reduce reactivity, particularly in circumstances involving densely loaded fuel zones where the moderator may fill all the space vacated.

Insertion of an axial, light-water-filled thimble into a D_2O flux trap (displacing D_2O) reduced reactivity. This reduction was not sufficient to cancel the gain for small D_2O flux traps. Consequently, it appeared that the installation of light water flux trap would increase reactivity up to a radius of 3 or 4 cm if the intermediate step (prior installation of a D_2O trap) were omitted.

The 5.1-cm-radius H_2O trap reduced reactivity quite effectively in a 28.6-cm-radius core, but it is not clear whether this would have been the case if the fuel zone had been larger. As may be seen in Fig. 5, there was a noticeably less favorable flux peak in the 28.6-cm core than was obtained in a 30.5-cm core enclosing the same H_2O flux trap. This would indicate a possibility that reactivity might be affected in a similar way.

V. COMPARISON OF ABSOLUTE FLUX AND FISSION RATE MEASUREMENTS WITH A CALCULATED RATIO

One of the major considerations in evaluation of various cores is the ratio of peak flux in the flux trap to power level in the core. Two measurements of absolute flux and fission rates were made in the $6A_0$ cores. The results agreed quite well with the ratio that was calculated for the same two points from foil-activation traverse data. Although sizeable corrections were included in the comparison, the technique is straightforward and well-known, and the agreement lends credence to the results presented in Table I. The tabulated values were the result of calculations utilizing the radial activation averages of the same tables, and disadvantage factors from References 3 and 9 for uniform lattice cores.

Flux trap foils were 0.584-cm-diameter, 0.0025-cm-thick gold. The product of thickness times macroscopic absorption cross section $\left(\overline{\Sigma}_a = 0.87 \times \Sigma_{a_{2200}}\right)$ was 0.0129 = τ_{Au}. Identical foils were irradiated in the Argonne Standard Pile (a radium-beryllium neutron source in graphite) at positions having known thermal flux and cadmium ratios. The relative (thermal) activations were measured and the absolute thermal neutron flux in the flux trap was estimated from the measured ratios. A 2200-m/sec equivalent flux of 1.36×10^8 was indicated by bare foil activities. However, subtraction of the epicadmium activation (CdR = 12) resulted in measured values of $\phi_{th} = 1.25 \times 10^8$ in runs 253-4 and 261-5. Flux perturbations by the foils nearly canceled, being estimated at 0.9681 in the Standard Pile, and 0.9685 in the D_2O flux trap. The term $[1/2 - E_3(\tau)]/\tau$ was estimated to be 0.969 in both locations,[10] where $E_3(\tau)$ is the exponential integral $\int_0^1 [\exp(-X)/X^3]dx$.

Fuel zone foils were 93% enriched in U^{235} and were 0.584 cm in diameter and 0.013 cm thick. Their weights were ~66 mg. Radiochemical measurements gave values of 9.87×10^{10} fissions per gram of bare uranium foil for 30 min run time The irradiation position experienced 1.33 times the average foil activation in the fuel zone midplane, and 1.33/2.4 times that of the flux trap peak where the flux was measured.

The expected fission rate calculated from the absolute flux measurement and the radial foil activation shapes was 9.88×10^{10} fissions per gram of uranium (93% enriched) in 30 min run time. The thermal flux $\phi = 1.25 \times 10^8 \times 0.64 \times 1.33/2.4 = 4.46 \times 10^7$ in the uranium foil location, including a flux perturbation estimate of 0.64. The estimates were based on a calculated value of $\tau = 0.3235$ and $[1/2 - E_3(\tau)]/\tau = 0.65$ for these foils. The expected thermal fission rate per gram of foil was calculated as follows:

$$\phi_{th} n \bar{\sigma}_f = 4.46 \times 10^7 \times (0.93/235) \times 6.023 \times 10^{23} \times 0.87 \times 582.2 \times 10^{-24}$$
$$= 5.38 \times 10^7 \text{ fissions/sec.}$$

Since the cadmium ratio was 52 (Reference 3, Table XXXVI), the bare activity should be 1.02 times the figure calculated above. The fast fission factor (ϵ) is taken to be unity. The estimate for a bare foil, irradiated for 1800 sec, is therefore

$$\text{No. of fissions per gram} = \epsilon \times 5.38 \times 10^7 \times 1.02 \times 1.8 \times 10^3$$
$$= 9.88 \times 10^{10}.$$

Conversion of the measured fission rate in a foil to that of the fuel zone requires division by the product of flux perturbation associated with the foil (0.64) times the fuel disadvantage factor (1.24 in the $6A_0$ fuel zone). This indicates a fission rate per gram of uranium fuel (93% enriched in U^{235}) of 1.26 times that in the foil. The U^{235} density was 2.86 g/liter of fuel zone, and the foil was located in 1.33 times the average midplane activation. The fission rate per liter of fuel zone averaged (at the midplane) was calculated as follows:

$$\text{No. of fissions per liter (per sec)} = 5.38 \times 10^7 \times 1.02 \times 1.26 \times 2.86/(0.93 \times 1.33)$$
$$= 1.6 \times 10^8.$$

The vertical flux shape for most cores would reduce the volume average to ~0.72 times the midplane average.

VI. EXTRAPOLATION TO ESTIMATED REACTOR POWER FOR 10^{16} PEAK THERMAL FLUX

Rough estimates were made of the reactor power required to produce a 10^{16} peak flux in the flux trap. These estimates applied ratio and proportion, with no effort to account for temperature and power coefficients. They indicate the general levels to be expected, and the trends, as various factors are adjusted.

Starting with the measured (and expected) fission rate from Section V for core 261-1, the following approximations were made: The measured

central peak thermal flux was 1.25×10^8, and the midplane average fission rate was 1.6×10^8 fissions per liter. By proportion, the power required to obtain a 10^{16} flux with a 3730-liter core operating at an average of 0.72 x the midplane power is

$$(10^{16}/0.781) \times 3730 \times 0.72/(3.1 \times 10^{16}) = \sim 1110 \text{ MW}.$$

Power levels for other cores were estimated by multiplying the volumes by the same specific power indicated above (i.e., 0.2976 MW/liter) and by the ratios between the two cores of fuel densities; of inverse disadvantage factors; and of inverse peak to average ratios. Disadvantage factors were obtained or deduced from References 1 and 3. The resulting values are tabulated in Table III.

Table III

EXTRAPOLATED POWER TO PRODUCE 10^{16} PEAK THERMAL FLUX

Loading	Disadvantage Factor	U^{235} Density	Volume of Fuel Zone (liters)	Estimated Power Level for 10^{16} Flux (MW)
399	1.28	199.0	59	418
398	1.28	199.0	70	468
397	1.28	199.0	54	357
395	1.28	199.0	59	549
394	1.28	199.0	87	420
367	1.20	25.74	412	621
365	1.20	25.74	395	559
361	1.20	25.74	387	494
359	1.20	25.74	329	561
358	1.20	25.74	315	652
271	1.20	25.74	406+	821
270	1.20	25.74	406-	693
269	1.20	25.74	407	631
268	1.20	25.74	291	603
266	1.20	25.74	263	473
265	1.20	25.74	272	549
264	1.20	25.74	285	728
263	1.20	25.74	308	1022
261	1.24	2.86	3731	1110
253	1.24	2.86	3471	1033
252	1.24	2.86	3322	989

VII. RISING PERIOD MEASUREMENTS OF INCREMENTAL WATER WORTH

Plots of reactivity worth of moderator ($d\rho/dH$-vs-H curves) indicated little effect attributable to an axial flux trap installed in $2A_0$ lattice cores fueled by 15/1 or 25/1 elements. Data points were indistinguishable between cores with and without flux traps except for two measurements with a core (No. 271) enclosing a trap having a 30.5-cm radius. These two points were about 10% higher than the curve approximating $d\rho/dH$ for the remaining data. Data for uniform lattice cores were from Reference 3. Data of $2A_0$ flux trap cores were selected from Table IV. The plot is shown in Fig. 13.

Table IV

RISING PERIOD MEASUREMENTS

Load-run No.	ΔD_2O Height	Initial D_2O Height	Rising Period (sec)	Approx* ρ	$\rho/\Delta H$
254-4'	0.762	113.82	41.51	0.001505	0.00198
261-4'	1.016	120.92	34.77	0.00167	0.00164
261-9'	0.889	122.81	44.80	0.00144	0.00162
264-1'	0.762	101.60	51.49	0.00132	0.00173
271-3'	1.524	124.94	25.23	0.0020	0.00131
271-4'	1.524	122.68	25.20	0.0020	0.00131
357-1'	1.320	131.70	37.47	0.0016	0.00121
358-1'	0.952	132.64	84.76	0.0009^+	0.00095
358-2'	1.727	132.64	37.92	0.0016	0.00093
361-3'	1.727	136.65	44.42	0.0015^-	0.00087
361-4'	1.283	137.01	71.02	0.0011^-	0.00086
364-1'	1.016	137.67	98.75	0.0008^+	0.00079
364-3'	1.333	139.42	69.75	0.0011^-	0.00071
365-1'	1.067	139.14	95.45	0.0009^-	0.00082
367-2'	3.048	161.90	45.05	0.0014^+	0.00046
397-2'	1.27	118.45	55.62	0.0013^-	0.00102

*A period-reactivity tabulation for cylindrical cores was used in converting rising period to reactivity.

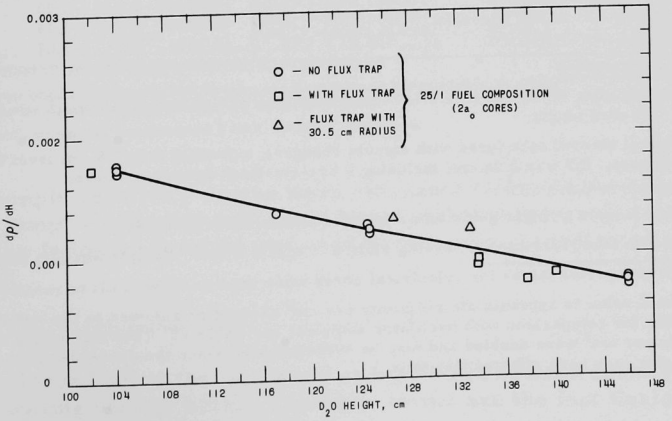

Fig. 13. Approximate Differential Water Worth Near Critical

VIII. APPROXIMATE WORTHS OF CADMIUM, D_2O, AND U^{235} SAMPLES

The worths of cadmium, D_2O, and U^{235} samples were measured in a few flux trap cores. The information was obtained to indicate relative worths of absorbing, fissionable, and moderating materials in various cores and at different locations in some of the cores.

A few samples were loaded for measurements of their effect on critical water height. The $d\rho/dH$ measurements of water worth (see Section VII) were used in converting these measurements to reactivity effects. Rising period-reactivity curves used in the $d\rho/dH$ measurements were for a uniformly loaded cylindrical core of $2A_0$ lattice spacing and were not modified to account for the presence of a flux trap. Little error is believed to result from this approximation. The measurements are tabulated in Table V.

Table V

CADMIUM SAMPLE WORTH
(Static)

Run No.	Location and Sample Type	Critical D_2O Height and Measured Change (cm)	Approx Reactivity*	Reactivity/cm^2 (x 10^4)	Adjusted Value** (x 10^4)
254-5, -6	Axial (A)	113.49 + 1.31	-0.0028	-1.63	-3.26
254-5, -7	Axial (B)	113.49 + 8.60	-0.0186	-1.37	-
254-1, -2	Axial (A)	113.49 + 1.30	-0.0028	-1.63	-3.26
260-1	81.3-cm radius (B)	111.87 + 1.19	-0.0026	-0.21	-
261-3	Axial (B) in flux trap	120.82 + 8.44	-0.0152	-1.03	-
261-4	Axial (C) in flux trap	120.82 + 0.11	-0.0002	-	-
261-9	79.25-cm radius (4xA)	121.16 + 1.65	-0.0030	-0.41	-0.82
261-12	63.50-cm radius (4xA)	121.16 + 4.66	-0.0084	-1.11	-2.22
266-3	Axial (D) in flux trap	117.07 + 6.93	-0.0109	-3.26	-6.52
271-3	Axial (A) in flux trap	121.26 + 3.68	-0.0048	-2.56	-5.12
271-4	35.56-cm radius (A)	121.26 + 1.42	-0.0019	-1.03	-2.06
364-1, -2	Axial (A) in H_2O flux trap	137.67 + 3.10	-0.0024	-1.14	-2.28
364-1, -3	18.1-cm radius (A)	137.67 + 1.75	-0.0014	-0.67	-1.34

Sample Descriptions

(A) Cadmium tube, 0.089-cm ID x 0.191-cm OD, having $\pi DL/4 = 0.15 \times L\ cm^2$. Sample was full core length.

(B) Cadmium sleeved tube (used with sample changer), extending from 38-cm level to top of core. OD was 2.06 cm, including 0.051-cm-thick cadmium sleeve; $\pi DL/4 = 1.62 \times L\ cm^2$.

(C) Voided sample changer guide tube without cadmium sleeve; see (B).

(D) Cadmium tube, 0.34-cm OD, having $\pi DL/4 = 0.27 \times L\ cm^2$. Sample was full core length.

*Reactivity-period tables for cylindrical cores were used to convert ΔH to reactivity.

**Adjusted value is approximate reactivity per cm^2 absorption adjusted to the midplane location for comparison with oscillator samples; see Table VI. (The full-length sample values per cm^2 were doubled and may be overestimated since the presence of a bottom reflector may have affected this term.)

Samples of highly enriched uranium, cadmium, and D_2O were stepped in and out of three critical cores for comparisons of their relative worths, as shown in Table VI. Reactivity was estimated on the basis of the amplitudes observed in a recorder trace of amplified and bucked current output from a boron-coated, ion current chamber as the samples were stepped in and out of the core with 10- or 15-sec waiting time. Although a "prompt jump" flux change following sample insertion of withdrawal is approximately linear with a small reactivity effect producing the change, it has the nature of a somewhat localized flux perturbation and may not produce identical responses in flux detectors that are not identically positioned relative to the sample and the core. Consequently, these data were compared to static measurements using the cadmium samples as a basis of comparison. For three comparisons with static measurements of cadmium tubing samples, ratios of 0.734, 0.645, and 0.500 were noted, the smallest value being obtained for a sample inserted at approximately 18-cm radius. (The flux detector remained at a single, fixed location outside the fuel zone during all measurements. The samples were all stepped to the same depth in the fuel elements regardless of moderator level.)

Table VI

OSCILLATED SAMPLE MEASUREMENTS

Run No.	Sample		Amplitude (%)	Reactivity (%)		Reactivity per Unit Sample	Ratio vs Static Measurement	Corrected to Static Measurement
	Location	Description		Total	Net			
266-4	(Axial, samples in D_2O flux trap)	Empty osc. can	-0.275	-0.01925	-	-	-	-
		Cd, 11.43 x 0.34-cm OD	-2.209	-0.154	-0.135	-4.79×10^{-4} ρ/cm²†	0.734	-6.52×10^{-4}
		D_2O, 22 g	+0.235	+0.01645	+0.0357	$+0.16 \times 10^{-4}$ ρ/g		$+0.22 \times 10^{-4}$
		U, enriched*	+0.892	+0.0624	+0.0817	$+3.27 \times 10^{-4}$ ρ/g		$+4.45 \times 10^{-4}$
364-5	(Axial, samples in H_2O flux trap)	Empty osc. can	-0.064	-0.00448	-	-	-	-
		Cd, 11.43 x 0.19-cm OD	-0.436	-0.03052	-0.0260	-1.47×10^{-4} ρ/cm²†	0.645	-2.28×10^{-4}
		D_2O, 22 g	-0.070	-0.00490	-0.0004	-0.00×10^{-4} ρ/g		-0.00×10^{-4}
		U, enriched*	+0.351	+0.02457	+0.0291	$+1.17 \times 10^{-4}$ ρ/g		$+1.81 \times 10^{-4}$
364-6	(Samples in fuel annulus**)	Empty osc. can	-0.023	-0.00161	-	-	-	-
		Cd, 11.43 x 0.19-cm OD	-0.193	-0.0135	-0.0119	-0.67×10^{-4} ρ/cm²†	0.500	-1.34×10^{-4}
		D_2O, 22 g	+0.018	+0.0126	+0.0142	$+0.065 \times 10^{-4}$ ρ/g		$+0.13 \times 10^{-4}$
		U, enriched*	+0.054	+0.00378	+0.00539	$+0.22 \times 10^{-4}$ ρ/g		$+0.44 \times 10^{-4}$

*Enriched uranium foil (93% U^{235}) wt, 2.495 g; dimensions, 10.16 x 0.95 x 0.013 cm.

** Sample changer located at 18.1-cm radius from axis of flux trap, inserting samples into guide tube in fuel annulus. Sample guide tube replaced one fuel pin from core. See Table V, notes B and C.

† Cadmium sample thermal cross sections estimated at $\pi DL/4$. See Table V, notes A and D.

Sample reactivity worths were estimated from measurements of the "prompt jump" associated with their insertion (or withdrawal) from the reactor. The following formula was used (a derivation is indicated in the appendix):

$$\Delta k/k = [\Delta n/n(0+)]\, \epsilon\beta .$$

The term $[\Delta n/n(0+)]$ is the measured change Δn in neutron density, divided by the resulting density $n(0+)$. The other terms are the fast fission factor ϵ

and the effective delayed neutron fraction β. These terms were taken to be unity and 0.07, respectively. The available measurements were instrument deflections which were linear with neutron flux leakage from the reactor in the vicinity of the flux detector.

IX. DESCRIPTION OF CORES AND FLUX TRAPS

A. Fuel Types

Three types of fuel were utilized for flux trap cores which used the same elements as those reported in Reference 3. These were designated by their atom ratios (Th/U^{235}), which were 15/1, 25/1, and 50/1. Diameters of fuel pellets were 0.660, 0.587, and 0.587 cm, respectively. Densities were 8.35, 8.655, and 8.476 g/cm^3. Weights of oxide per fuel element were estimated to be 434.6, 357.2, and 349.8 g. This was broken down to content of thorium, uranium, U^{235}, and oxygen, as follows:

(15/1 fuel) 434.6 g = 355.9 g Th + 25.85 g U (24.04 g U^{235}) + 52.8 g O_2;

(25/1 fuel) 357.2 g = 300.51 g Th + 13.25 g U (12.35 g U^{235}) + 43.4 g O_2;

(50/1 fuel) 349.8 g = 300.6 g Th + 6.66 g U (6.21 g U^{235}) + 42.5 g O_2.

Nominal lengths of the stacked pellet columns were 152.4, 152.6, and 152.6 cm. The 15/1 fuel was contained in nominal 0.793-cm OD, Type 1100 aluminum tubing of 0.036-cm wall thickness and 155.3-cm length. Based on a weight of 34.49 g, the inside and outside diameters were estimated to be 0.718 and 0.787 cm, respectively. The top and bottom plugs were Type 6061 aluminum weighing 2.0 and 2.5 g. The 25/1 and 50/1 fuel were contained in nominal 0.793-cm OD, Type 1100 aluminum tubing of 0.081-cm wall thickness and 154.62-cm length. Based on a weight of 81.525 g, the inside and outside diameters were estimated to be 0.610 and 0.787 cm. The top and bottom plugs were Type 6061 aluminum, weighing 2.1 and 2.5 g.

Spectrochemical analyses indicated no significant variation from the nominal amounts of impurities in the aluminum tubing.

B. Lattice Spacings

Lattice spacings were A_0 (0.953 cm or 3/8 in.), $2A_0$, $3A_0$, and $6A_0$, all being based on an equilateral, triangular lattice in the same grid.

C. Fuel Zone Dimensions

Fuel zone dimensions were measured and also estimated from the cell areas and from the number of fuel elements loaded. Since the triangular lattice spacing did not produce smoothly curved fuel zone boundaries, there were locations where the fuel zones deviated by half a lattice space in one

or both edges, from the stated radii. Typical fuel zone boundaries were formed by swinging an arc with a pointer fastened to a (temporary) central pin on the axis of the flux trap. Any fuel element reached by this pointer would then be removed, if changing an inner boundary, or retained, if changing an outer boundary.

The values for effective inner and outer radii of annular fuel zones were based on calculations of the radii of cylinders of the same cross-sectional area as the given number of cells. The number of cells was the number of fuel elements in the fuel zone, or the number of vacant positions within the flux trap. The area per cell was 0.433 x (lattice spacing)^2.

D. Flux Trap Dimensions

Flux traps were formed by removing fuel from the vicinity of the core axis, or by loading annular fuel zones, etc. Flux traps ranged in size up to 104 x 104 cm. Effective radii of cylindrical D_2O flux traps were calculated on the basis of equivalent cross-sectional areas for the number of vacant cells (i.e., number of fuel elements removed to form the trap). Actual boundaries were somewhat irregular and varied by as much as half a lattice space about the effective figure. This variability was inherent in the use of a triangular grid pattern in approximating cylindrical geometry. The D_2O height in the core was the same as that in the flux trap.

H_2O flux traps were constructed by inserting H_2O-filled thimbles through axial grid openings, thus displacing D_2O from the trap region during reactor operation. At least a small D_2O region always remained between each H_2O thimble and the annular fuel zone. The H_2O level was roughly the same as that of the D_2O in the core.

E. Description of Fuel Zones

The more important features of the fuel zones are summarized in Table VII.

Table VII

DESCRIPTION OF FUEL ZONES

Fuel Ratio (U^{235}/Th^{232})	Lattice* Pitch (cm)	Fuel Pellet Radius (cm)	Cell Size (cm^2)	U^{235} Density (g/liter)	$\sim\bar{\Sigma}_a$	$\sim\bar{\Sigma}_f$
25/1	5.715	0.2972	28.28	2.86	0.0051	0.0031
25/1	2.858	0.2972	7.06	11.46	0.0191	0.0120
25/1	1.905	0.2972	3.14	25.74	0.0406	0.0259
15/1	1.905	0.3302	3.14	49.79	0.0628	0.0445
15/1	0.953	0.3302	0.786	199.0	**	**

*Triangular lattice spacing.

**Because of the variation in neutron energy spectrum in the thin fuel zones having $1A_0$ lattice spacing, no estimate of Σ_a or Σ_f was made, since these are spectrum-dependent and vary with radius.

APPENDIX

Derivation of Formula for Estimation of Reactivity Changes by Measurement of Prompt Jump in Neutron Density

The approximate reactivity worth of a sample may be evaluated from the "prompt jump" in neutron density which accompanies stepwise sample insertion into (or withdrawal from) a reactor. Such measurements have been used with numerous adaptations and varying degrees of sophistication at various sites. The derivations that follow started with Equation 25 Reactor Handbook (Physics) AECD-3645, p. 537, Ch. 1.6, or with Equation 5.25 of Reactor Handbook, Second Edition (Interscience Publishers), Vol. III, Part A. The equations involve neutron densities n(t) at times zero and zero + (just before and just after a step reactivity input), the effective multiplication constant k, fast fission factor ϵ, and effective delayed neutron fraction β. Only algebraic manipulation is required. The two reference equations lead to slightly different results.

Equation 25 is

$$n(0+) = \frac{n(0)}{k} \frac{1}{1 - (k-1)/(k\epsilon\beta)}.$$

Substituting $1 + \Delta k$ for k, and $n(0+) - \Delta n$ for n(0) results in

$$\Delta k = \frac{\Delta n}{n(0+)} \frac{\epsilon\beta}{1 - \epsilon\beta} = \frac{\Delta n}{n(0)} \frac{\epsilon\beta F}{1 - \epsilon\beta},$$

where

$$F = n(0)/n(0+).$$

Variously, one may solve for k ($k = 1 + \Delta k$) or for $\rho = \Delta k/k$, as follows:

$$\rho = \frac{\Delta k}{k} = \frac{\Delta n}{n(0+)} \frac{\epsilon\beta}{1 - \epsilon\beta F} = \frac{\Delta n}{n(0)} \frac{\epsilon\beta F}{1 - \epsilon\beta F},$$

or

$$\rho \doteq [\Delta n/n(0+)]\epsilon\beta.$$

If one starts with Equation 5.25 instead of Equation 25, slightly different results are obtained. Equation 5.25 is

$$N_1/N_0 = n(0+)/n(0) = 1/(1 - \rho/\beta)$$

$$\rho = \Delta k/k = [\Delta n/n(0+)]\ \beta.$$

The ratio between the two estimates of ρ is therefore $\epsilon/(1 - \epsilon\beta F)$, or approximately $\epsilon \cdot (1 + \epsilon\beta F)$. Since ϵ is near unity in the cores considered in this report, the two results are nearly equal.

ACKNOWLEDGMENT

The following personnel participated in the experiment. W. C. Redman defined the goals of the experiment and conferred frequently as it progressed. Subsequently, E. M. Pennington compared the observed data with analytical results. S. G. Kaufmann supervised the ZPR-VII facility which was staffed, for these experiments, by Q. L. Baird* and K. E. Plumlee, physicists; J. W. Armstrong, technical assistant; W. R. Robinson** and P. J. Durand,† technicians; and C. E. Ward, a student assistant on the Northwestern University cooperative plan. C. E. Ward measured the absolute flux, and R. J. Armani supplied absolute fission rate measurements. W. R. Robinson and P. J. Durand made many of the foil activation measurements. I. K. Olson and W. R. Robinson assisted in the preparation of this report.

---

* Now with Idaho Operations Office, AEC.

** Now technical assistant.

† Now with Atomics International.

REFERENCES

1. E. M. Pennington, Calculations for ZPR-VII Flux-Trap Reactors with Heavy Water-Moderated Cores, ANL-6406 (August 1961).

2. K. E. Plumlee and S. G. Kaufmann, Flux to Fission Rates in Annular Cores, Trans. Am. Nucl. Soc. 2 (1) 166-167 (June 1959).

3. W. C. Redman, S. G. Kaufmann, K. E. Plumlee, and Q. L. Baird, Critical Experiments with Thoria-Urania Fuel in Heavy Water, ANL-6378 (December 1961).

4. J. W. L. DeVilliers, Editor, Critical Experiments for the Preliminary Design of the Argonne High Flux Reactor, ANL-6357 (June 1961).

5. J. W. L. DeVilliers, Q. L. Baird, J. Juliano, C. N. Kelber, R. Kiyose, and K. E. Plumlee, Critical Experiments for the Preliminary Design of the Argonne High Flux Reactor, Part A, Trans. Am. Nucl. Soc. 4 (1) 109 (June 1961).

6. J. O. Juliano, C. N. Kelber, and K. E. Plumlee, Critical Experiments for the Preliminary Design of the Argonne High Flux Reactor, Part B, Trans. Am. Nucl. Soc. 4 (1) 110 (June 1961).

7. M. S. Silberstein, Argonne Advanced Research Reactor, UNC-5024 (July 1962).

8. K. E. Plumlee and M. T. Wiggins, Automatic Foil Activity Counting Facility and Data-reduction Program, ANL-6628 (October 1962).

9. E. M. Pennington, Calculations for ZPR-VII Uniform Lattice Critical Experiments with Thoria-Urania Fuel in Heavy Water, ANL-6661 (December 1962).

10. F. H. Helm, Numerical Determination of Flux Perturbation by Foils, Nucl. Sci. and Eng. 16, 235-238 (1963).